**P4.4** SIMULATIONS OF PRESENT-DAY TROPICAL CYCLONE CLIMATOLOGY AND THEIR TEMPORAL VARIABILITY ASSOCIATED WITH ENSO WITH A 20-KM-MESH HIGH-RESOLUTION AGCM

Hiroyuki Murakami*[1], Jun Yoshimura[2], Bin Wang[3]
[1]Advanced Earth Science & Technology Organization / Meteorological Research Institute, Ibaraki, Japan
[2] Meteorological Research Institute, Ibaraki, Japan
[3] Department of Meteorology, University of Hawaii

## 1. INTRODUCTION

Tropical cyclones (TCs) are among the most harmful weather phenomena. Recently, a number of studies have been conducted using global circulation models (GCMs) to explore the influence on TC activity of global warming associated with warmer sea surface temperatures and increased-$CO_2$. For example, Oouchi et al. (2006) evaluated TC changes in a warm-climate environment using a 20-km-mesh, high resolution GCM. They concluded that, globally, the frequency of strong-intensity TCs would increase, while the total frequency of TCs would decrease. They insisted that their simulation results were much more reliable than those of other studies because of the use of the high resolution GCM. They carefully evaluated the reliability of their projection of TCs by comparing their present-day 10-year, experimental data with observational data for geographical distribution, frequency, and intensity. However, because they used 10-year averaged boundary conditions as a present climate experiment, it is uncertain whether the GCM can reproduce real TCs given the observational sea-surface temperature (SST) and sea-ice concentration (SIC).

The goal of this study was to evaluate the TC simulation of seasonal variability of genesis position, interannual variability, and trend with the same GCM used by Oouchi et al. (2006) under the present-climate condition using an observational SST and SIC. In this study, we also evaluated the GCM performance of the dependence of TC activity on the El Niño-Southern Oscillation (ENSO) in the Western North Pacific (WNP) basin in terms of position of TC genesis and difference of accumulated cyclone energy (ACE).

## 2. MODEL DESCRIPTION AND EXPERIMENTAL DESIGN

The GCM used in this study is the Japan Meteorological Agency (JMA) and Meteorological Research Institute (MRI) Atmospheric GCM (hereafter referred to as "JM-AGCM"), the same GCM used by Oouchi et al. (2006). The resolution is TL959L60 (i.e., triangular truncation 959 with the linear Gaussian grid equivalent to 20-km mesh horizontally and 60 layers vertically). The dynamical core is the same as that of the JMA operational global spectral model (GSM) (JMA, 2007), which is hydrostatic, spectral, and anelastic. The physics are mostly the same as those of the GSM, but they are optimized for climate simulations. The details of the optimization are available in Mizuta et al. (2006).

The simulation conducted in this study was forced with the known observational global SST and SIC, namely, the Hadley Centre sea-ice and sea-surface temperature data set version 1 (HadISST1) (Rayner et al., 2003), as lower boundary conditions. The simulation started from May of 1978. After an 8-month spin-up run, a consecutive integration for 25 years (1979-2003) was implemented.

The method of TC identification involved the six sets of criteria described in Oouchi et al. (2006). As an observational data set for TCs, a global TC best-track data set was used. The data set was obtained from the Unisys Corporation website (Unisys, 2008), which contains the historical observed TC tracks from 1979 to 2003.

## 3. RESULTS

### 3.1 *TC GENESIS, INTENSITY, AND DURATION*

Figure 1 shows the locations of TC genesis and tracks them seasonally. In general, the JM-AGCM captures very well observational features, namely, the latitudinal and longitudinal distribution of genesis position and the seasonal variability for each basin. However, when viewed in detail, there are too many TCs at lower latitudes of the Southern Hemispheric Indian Ocean (around 30-80°E) and along the coast of Brazil. The frequency of TCs in the lower latitudinal area of the WNP basin (10-15°N and 120°E-160°E) is underestimated, as reported in (Oouchi et al., 2006). The frequency of TCs in the high-latitude area of the North Atlantic Ocean basin (around 25-35°N ) is also underestimated.

For the evaluation of the intensity and duration of TCs, the probability density of the maximum wind speed and duration is shown in Figure

* *Corresponding author address:* Meteorological Research Institute 1-1 Nagamine, Tsukuba, Ibaraki, Japan, 305-0052; e-mail: himuraka@mri-jma.go.jp

2, along with records of maximum wind speeds of more than 17 m/s (stronger than the category of "Tropical Storm"). As for the probability density of the maximum wind speed, the JM-AGCM tends to underestimate a strong maximum wind speed compared with the observation. Although the observation shows that more than 10 percent of TCs develop maximum wind speeds of up to 50 m/s, the JM-AGCM seems to be limited to intensifying such strong wind speeds. The duration probability density also seems to be underestimated by the JM-AGCM in that the TC lifetime is too short, although the overall features of the duration seem to be well simulated.

### 3.2 *TREND AND INTERANNUAL VARIABILITY OF GENESIS FREQUENCY*

In order to evaluate the interannual variability of genesis frequency (i.e., trend and correlation of detrended variability) obtained by the JM-AGCM, we compared it with the observed variability. A summary is shown in Table 1. For the genesis trend analysis, we used Mann-Kendall rank statistics (Kendall, 1938). In Table 1 are shown the trend values of all TCs and of TCs with a recorded maximum wind speed of more than 32.0 m/s (i.e., Typhoon Category). For all TCs, no significant trends are seen over comprehensive areas (e.g., global, Northern Hemisphere, and Southern Hemisphere) by either observation or the JM-AGCM. It is also notable that the trends idendified by the JM-AGCM are similar to those observed. However, there is no consistent sign of trend for each ocean basin, and no significant trends can be seen for either of them. Similarly, there is no consistent sign of trend for wind speeds of more than 32.0 m/s. Although the negative trend of the North Indian Ocean basin is statistically significant according to the JM-AGCM, most of the trends are not statistically significant. For evaluation of the detrended interannual variability by the JM-AGCM, Table 1 also shows correlations between the observation and the JM-AGCM, in which a linear trend is subtracted. For all TCs, there are no statistically significant correlations. However, for wind speeds of more than 32 m/s, there are higher correlations than those found for all TCs. The global and North Atlantic Ocean basin statistics show statistically significant correlations. It can be inferred that the JM-AGCM can simulate the interannual variability for strong TCs.

### 3.3 *Interannual variability influenced by ENSO*

The interannual variability of TCs influenced by ENSO was investigated. Here, El Niño and La Niña years are defined by (Camargo and Sobel, 2005): the El Niño years are 1982, 1986, 1987, 1991, 1994, 1997, and 2002, and the La Niña years are 1988, 1995, 1998, and 1999. Figure 3 shows genesis positions and tracks of TCs for each ENSO phase. The observation data reveal that genesis positions during the El Niño years shift southeastward, while those during the La Niña years shift northwestward, as also reported by Wang and Chan (2002). The JM-AGCM simulation data reveal a subtle southeastward shift during the El Niño years though there are fewer TCs around the lower latitude and eastern area (e.g., around 140-175°E, 5-15°N).

In order to evaluate the variability of TC activity influenced by ENSO, accumulated cyclone energy (ACE; (Bell et al., 2000); (Camargo and Sobel, 2005)) is the focus here. ACE is a quantity defined as follows,

$$ACE = \sum (Vmax)^2 \quad (when \quad |Vmax| \geq 17m/s), \quad (1)$$

where $Vmax$ is the sustained maximum wind velocity. The ACE is the sum of the squares of the estimated 6-hourly maximum sustained surface wind velocity only when $Vmax$ exceeds 17 m/s, which corresponds to the tropical storm intensity. When there are stronger and longer TCs, the ACE increases. Figure 4 shows the time series of the ACE as well as three deviation indices, namely, TC number, duration in which the maximum wind speed is more than 17 m/s, and the averaged maximum wind speed. These time series are plotted for each year between 1979 and 2003 over the WNP basin (100°E-180, 0-60°N). As (Camargo and Sobel, 2005) pointed out, the observed ACE values are larger in the El Niño years but smaller in the La Niña years, which are related to the three indices. As for the JM-AGCM simulation, the ACE in the El Niño years is also larger than in the other years, although the ACE itself is underestimated compared with the observation because both the genesis frequency and duration given by the JM-AGCM are underestimated compared with the observation (see Figure 2). In the strong El Niño years of 1994 and 1997, the observation shows the largest genesis frequency, whereas the model cannot simulate the tendency. However, the model indicates the increased duration and average maximum wind speed in the El Niño years, which are well described by the observation. These increases cause the ACE identified by the JM-AGCM in El Niño years to be larger than in other years. The longer duration in the El Niño years identified by the JM-AGCM must be associated with the southeastward shift of the averaged genesis position. Although the observation shows a smaller ACE in the La Niña years, the JM-AGCM does not show a sig-

nificant decrease. Perhaps this is because the genesis frequency is not well correlated with the ENSO by the JM-AGCM, although it seems to be relatively well correlated with the observation data collected after 1990. Because (Wang and Chan, 2002) reported that the total number of TCs formed in the WNP basin did not show a significant ENSO influence, it is uncertain whether the genesis frequency is correlated with ENSO. Moreover, the fluctuations of all three indices are well synchronized after 1990 in the observation. As for the JM-AGCM, the duration and averaged maximum wind speed are well synchronized, though the genesis frequency does not follow, which highlights the need for a great improvement in measuring the interannual variability of genesis frequency in order to simulate TC activity influenced by ENSO.

## 4. SUMMARY AND CONCLUDING REMARKS

We conducted a 25-year, present-day simulation with a 20-km-mesh JM-AGCM using observational SST and SIC as lower boundary conditions in order to evaluate the model performance of interannual and seasonal variabilities of the genesis position and genesis frequency of TCs. For validation, we used best-track data provided by Unisys. The results show that the genesis position and its seasonal variability for each basin are quite realistic, though TCs over the WNP basin and high-latitude North Atlantic basin are underestimated. The maximum wind speed and duration in which the maximum wind speed exceeds 17m/s are also underestimated compared with the observation.

Interannual trends of TC frequency were also examined. Neither the JM-AGCM nor the observation shows a significant trend. Analysis of a detrended correlation between the JM-AGCM experiment and observation shows that the correlation increases when they are analyzed for only the strong wind speed category of TCs.

The interannual variability of TCs influenced by ENSO was also investigated in terms of accumulated cyclone energy (ACE). Although the ACE value by the JM-AGCM is underestimated compared with the observation, the general feature indicating that the ACE increases in El Niño years is well simulated because the JM-AGCM simulates well the tendency toward a southeastward shift of the genesis position and a longer duration in which the maximum wind speed exceeds 17m/s in the El Niño years.

Overall, these results indicate that the JM-AGCM captures observational features in terms of trend, seasonal variability of genesis position, and interannual variability influenced by the ENSO. It is surprising that these features are largely captured given only the lower boundary conditions with the high-resolution AGCM.

Further work must be done to overcome the lack of genesis numbers over the WNP. Further evaluation of the required horizontal resolution must also be undertaken to resolve and simulate the observational wind intensity. Atmosphere-ocean interactions also must be considered when the TC intensity is evaluated.

## 5. ACKNOWLEDGMENTS

This was conducted under the framework of the ”Projection of the change in future weather extremes using super-high-resolution atmospheric models,” supported by the KAKUSHIN Program of MEXT. The authors would like to thank Dr. Akira Noda and Dr. Kazuyoshi Oouchi of the Frontier Research Center for Global Change (FRCGC) for their support with regard to this study. We also thank the Earth Simulator Center for providing computational environments.

## REFERENCES

Bell, G. D., M. S. Halpert, R. C. Schnell, R. W. Higgins, J. Lawrimore, V. E. Kousky, R. Tinker, W. Thiaw, M. Chelliah, and A. Artusa, 2000: Climate assessment for 1999. *Bull. Amer. Meteor. Soc.*, **81**, S1–S50.

Camargo, S. J. and A. H. Sobel, 2005: Western North Pacific tropical cyclone intensity and ENSO. *J. Climate*, **18**, 2996–3006.

JMA, 2007: Outline of the operational numerical weather prediction at the Japan Meteorological Agency. 194 pp.

Kendall, M. G., 1938: A new measure of rank correlation. *Biometrika*, **30**, 81–93.

Mizuta, R., K. Oouchi, H. Yoshimura, A. Noda, K. Katayama, S. Yukimoto, M. Hosaka, S. Kusunoki, H. Kawai, and M. Nakagawa, 2006: 20-km-mesh global climate simulations using JMA-GSM model -mean climate states-. *J. Meteor. Soc. Japan*, **84**, 165–185.

Oouchi, K., J. Yoshimura, H. Yoshimura, R. Mizuta, S. Kusunoki, and A. Noda, 2006: Tropical cyclone climatology in a global-warming climate as simulated in a 20km-mesh global atmospheric model: Frequency and wind intensity analyses. *J. Meteor. Soc. Japan*, **84**, 259–276.

Rayner, N. A., D. E. Parker, E. B. Horton, C. K. Folland, L. V. Alexander, and D. P. Rowell, 2003:

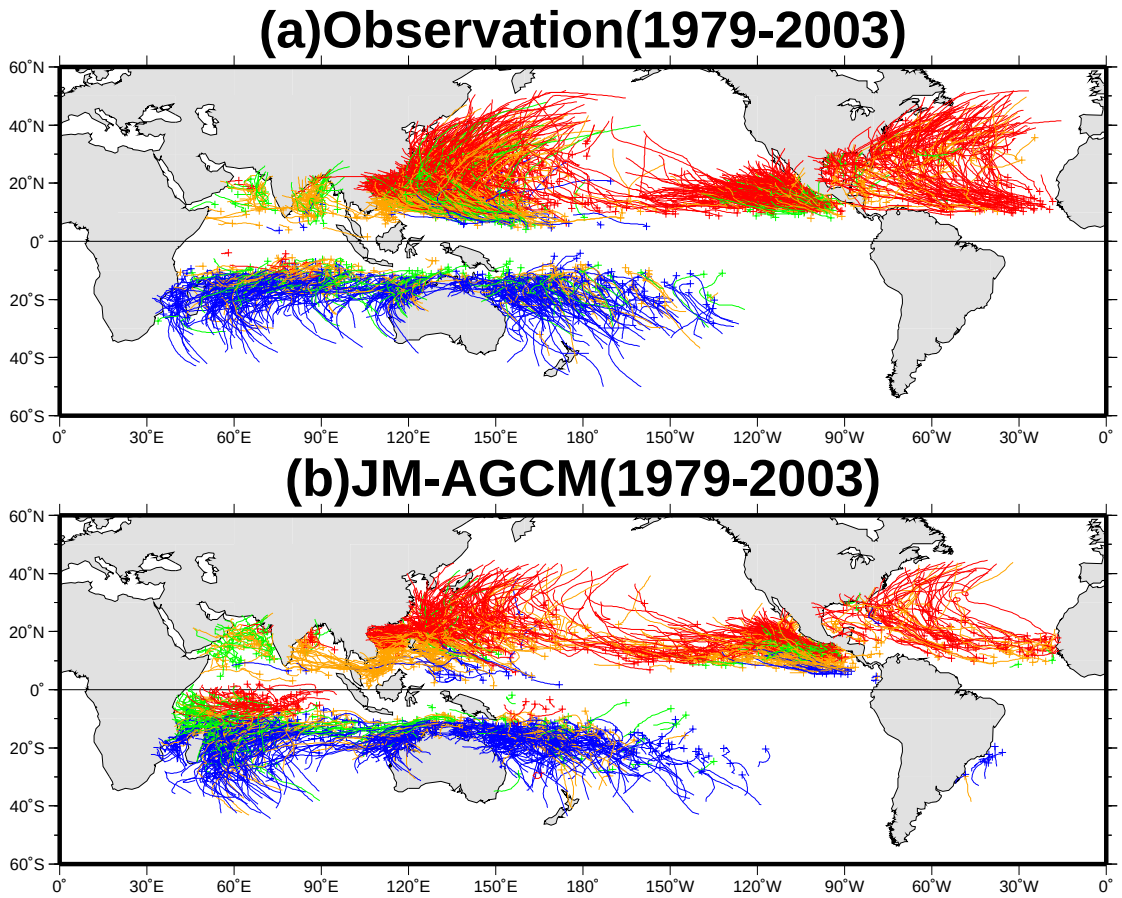


FIG. 1: TC genesis location and track by (a) observation and (b) JM-AGCM. The initial positions are marked with + signs. The colored lines express different seasons: blue for January, February, and March; green for April, May, and June; red for July, August, and September; orange for October, November, and December.

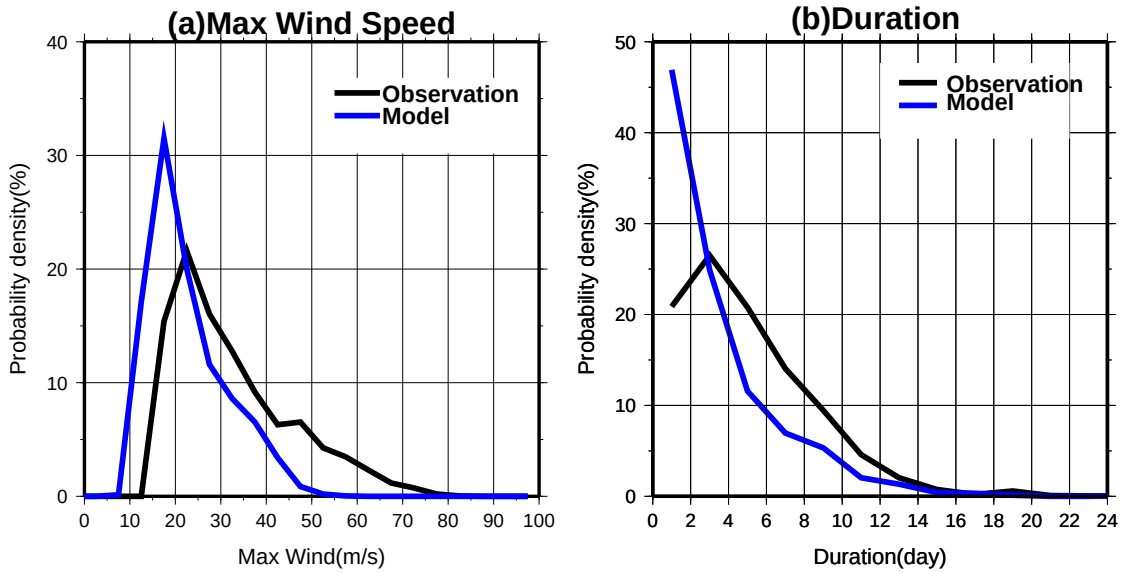


FIG. 2: Probability density of (a) maximum wind speed (m/s) and (b) duration (days) on which maximum wind speeds of more than 17m/s were recorded. The black and blue lines show the observation and model, respectively.

Table 1: Summary of genesis interannual variability

| Area | All TCs | | | Over 32.0m/s | | |
|---|---|---|---|---|---|---|
| | Obs Trend | AGCM Trend | D.Corr.$^{+}$ | Obs Trend | AGCM Trend | D.Corr.$^{+}$ |
| Global | 0.15 | 0.16 | 0.23 | 0.11 | 0.05 | 0.44$^{*}$ |
| Northern Hemisphere | 0.09 | 0.03 | 0.13 | 0.01 | -0.05 | 0.39 |
| Southern Hemisphere | 0.09 | 0.15 | 0.10 | 0.08 | 0.04 | 0.51 |
| North Indian Ocean[a] | -0.11 | -0.09 | 0.14 | 0.02 | -0.37$^{*}$ | -0.28 |
| Western North Pacific Ocean[b] | 0.05 | -0.22 | 0.27 | -0.01 | -0.23 | 0.33 |
| Eastern North Pacific Ocean[c] | -0.17 | 0.11 | -0.11 | -0.28 | 0.03 | 0.18 |
| North Atlantic Ocean[d] | 0.27 | 0.15 | 0.19 | 0.08 | -0.25 | 0.56$^{*}$ |
| South Indian Ocean[e] | 0.07 | 0.15 | 0.14 | 0.22 | 0.07 | 0.29 |
| South Pacific Ocean[f] | -0.13 | 0.04 | -0.08 | -0.22 | -0.17 | 0.07 |

[a] Longitude=30 E-100 E
[b] Longitude=100 E-180
[c] Longitude=180-90 W
[d] Longitude=90 W-0
[e] Longitude=20 E-135 E
[f] Longitude=135 E-90 W
$^{*}$ Statistically significant at 95% confidence level.
$^{+}$ Detrended correlation between the observation and the JM-AGCM.

Global analyses of sea surface temperature, sea ice, and night marine air temperature since the late nineteenth century. *J. Geophys. Res.*, **108**, 2–1 – 2–30.

Unisys, 2008: Unisys weather hurricane tropical data. [Available online at http://weather.unisys.com/hurricane/].

Wang, B. and J. C. L. Chan, 2002: How does ENSO regulate tropical storm activity over the Western North Pacific? *J. Climate*, **15**, 1643–1658.

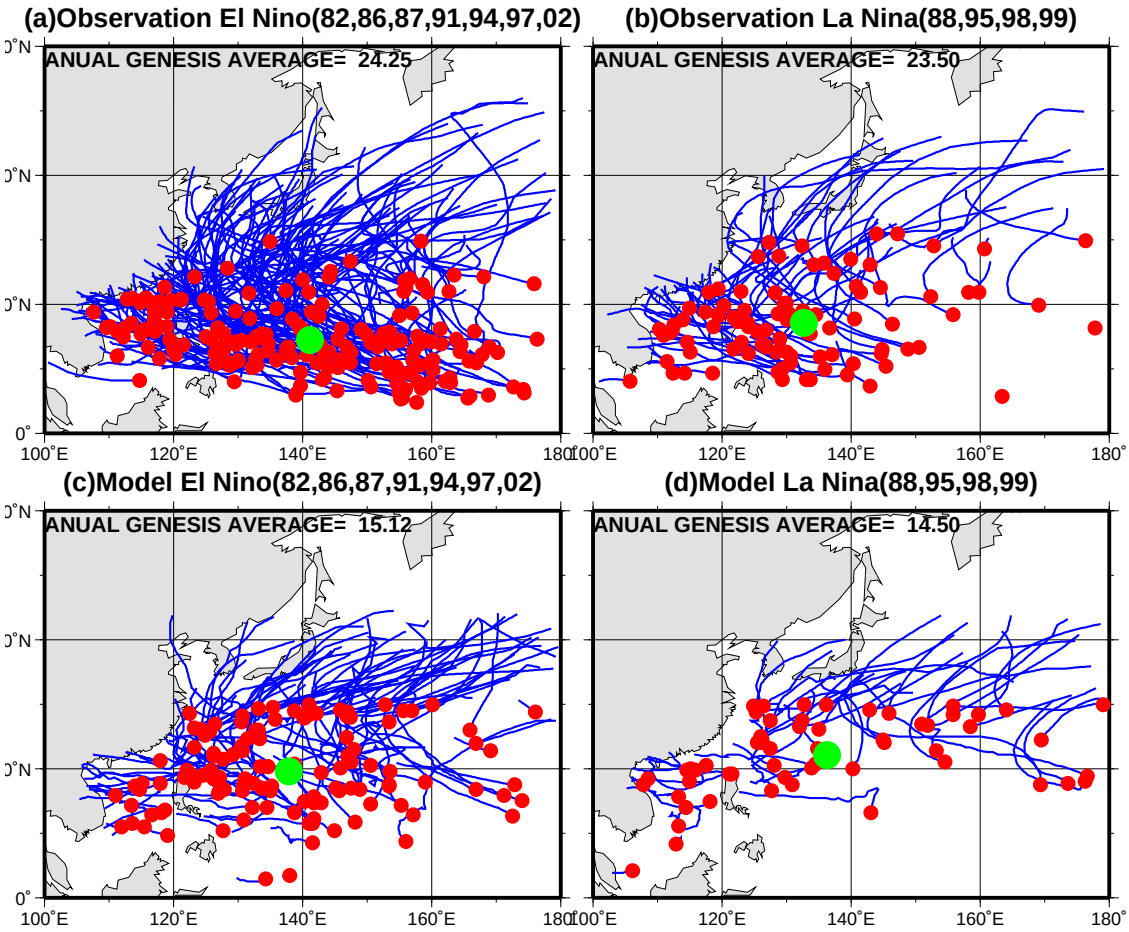


FIG. 3: TC genesis positions and tracks for each (a) observation in El Niño, (b) observation in La Niña, (c) model result in El Niño, and (d) model result in La Niña. Red plots show genesis positions. Blue lines show tracks. Green plots show average genesis positions.

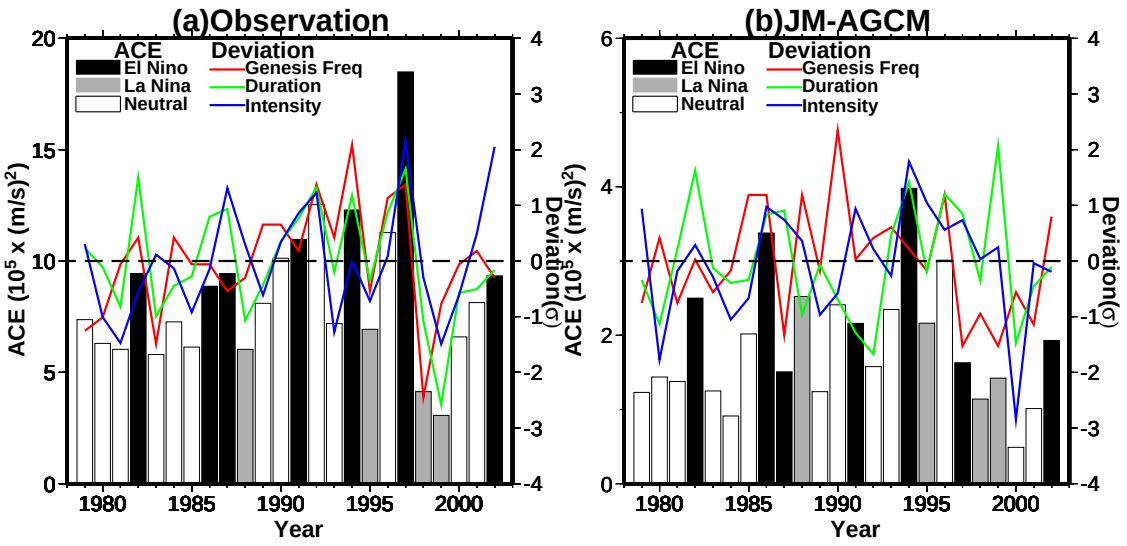


FIG. 4: ACE per year between 1979-2003 for (a) observation and (b) JM-AGCM. Black, gray, and white bars show El Niño, La Niña, and neutral years, respectively. The colored lines show the deviation of genesis frequency (red), duration in which maximum wind speed exceeds 17m/s (green), and averaged maximum wind speed (blue). Note that the vertical scale is different between the panels.